Heat transfer in reactive Co/Al nanolaminates

M. L. Hobbs[1], D. P. Adams[2] & J. P. McDonald[2]
[1]*Nanoscale & Reactive Processes, Sandia National Laboratories, USA*
[2]*Thin Film, Vacuum & Packaging, Sandia National Laboratories, USA*

Abstract

Reaction front propagation rates of free standing multilayer thin foils of Co/Al have been determined using a diffusion limited reaction model by means of a method-of-lines code with a stiff solver and adaptive gridding. Predicted and measured reaction front speed variations with bilayer thickness, t_b, can be separated into three regimes. The three regimes are delineated by the critical bilayer thickness, $t_{b,c}$, and the bilayer thickness that produces the maximum front velocity, $t_{b,max}$. The critical bilayer is composed predominately of premixed or fully reacted Co_xAl_y with a thickness of ~2.7 nm. The front velocity in the three regimes 1) is zero when $0 \le t_b \le t_{b,c}$ since there are no reactants 2) increases when $t_{b,c} < t_b < t_{b,max}$ since the reactant concentration increases with t_b and 3) decreases when $t_{b,max} < t_b$ since the diffusive resistance increases with t_b. The sensitivity of front velocity to property variation is discussed. Steady and oscillatory combustion are predicted for this material pair.

Keywords: Co/Al, gasless metal combustion, diffusion, nanolaminate.

1 Introduction

Alternating nanoscale layers of pure metals can be ignited to produce localized and rapid heating for improved soldering or brazing of microelectronic assemblies [1]. Exothermic metal multilayers used for these applications consist of hundreds or thousands of individual reactant layers generally having a single out-of-plane periodicity. Figure 1.A shows a cross section of a multilayer nanolaminate of Co and Al deposited by direct current sputtering [2]. The layer periodicity is uniform through thickness and the metal layers are high-purity, polycrystalline metal. As shown in Figure 1.B, a 27 Å thick premixed Co_xAl_y interlayer forms at the interfaces between the Co and Al layers.

WIT Transactions on Engineering Sciences, Vol 61, © 2008 WIT Press
www.witpress.com, ISSN 1743-3533 (on-line)
doi:10.2495/HT080121

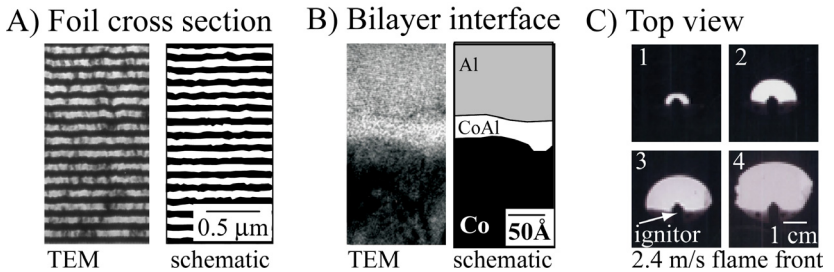

Figure 1: A) Example foil cross section showing multiple bilayers, B) evidence of amorphous Co_xAl_y layer between the Co and Al layers, and C) plan view of foil during reaction. Transmission electron microscopy (TEM) was used for A and B and high-speed photography in C.

Foils of various design exhibit self-propagating high temperature synthesis. Reaction occurs whether ignited in air (as part of the current study) or in vacuum. Figure 1.C shows a plan view of a thin multilayer nanolaminate at various times after single point ignition. Detached foils were ignited over the apertures of metal washers. The reacted portion of the foils is lighter in color than the unreacted portion.

In this proceeding, we model the dynamics of self-propagating high temperature synthesis as a function of multilayer design. In general, the trends in the current work are consistent with previous work involving other exothermic material pairs [3]. All of the foils are free standing in the current work. The behaviour of nanolaminates reacted on a substrate is discussed in reference [4].

2 Diffusion limited reaction model

Hardt and Phung [5] developed an analytical model for propagation of gasless reactions in solids. This model was developed for binary metal powder mixtures by assuming that the metals were one dimensional (layered) and that the thermophysical properties were independent of temperature. Hardt and Phung further assumed that melting of the reactants do not affect the burning process and that the specimen is large compared to the front width. These assumptions imply that heat loss by radiation or convection from the surface of the specimen does not disturb the internal temperature in or near the reaction zone.

In the current work, reactive foils are modelled as a continuum since the dimensions of the foils are too small to model discretely. For example, to discretize the thickness of the mixed Co_xAl_y layer shown in Figure 1.B with three elements would require billions of elements to model the complete system shown in Figure 1.C, even as a 2D axisymmetric system. Furthermore the time steps would be prohibitively small. The continuum assumption allows the reactive nanolaminates to be modelled with a constitutive model similar to the model described by Hardt and Phung [5].

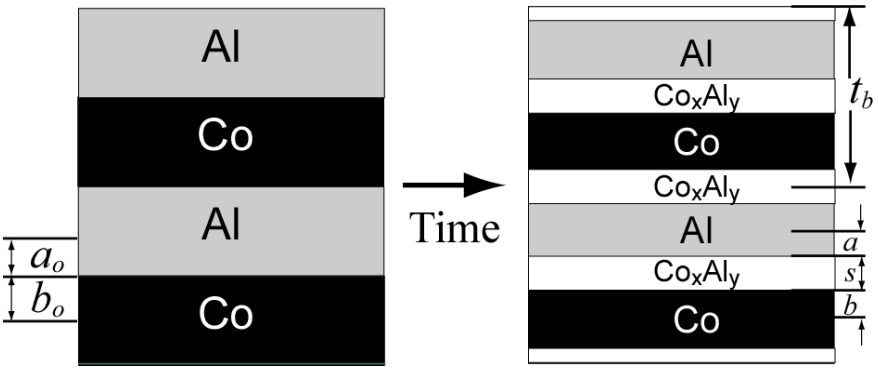

Figure 2: Two bilayers of Al and Co showing initial half thicknesses a_o and b_o, with $t_b = 2(a + b + s)$. After time a mixed layer s with composition Co_xAl_y is formed between the Al and Co layers.

Figure 2 shows a cross section of two bilayers with a, b, and s representing the half thickness of phase A and B, and the full thickness of the mixed layer s. For example, A represents aluminium, B represents cobalt, and s represents the mixed or fully reacted layer Co_xAl_y. The subscript "o" denotes the layer thicknesses before the initial interfacial layer is formed. The "initial" interfacial layer thickness is represented by s_i and is assumed to be constant. The initial thicknesses of the material A and B are determined once the initial thickness of the reacted layer, s_i, is specified.

A one-dimensional (1D), multiple layer, method-of-lines temperature based chemistry code, Tchem, has been developed for spherical, cylindrical, or slab geometries with a general library for inert and reactive nanolaminate materials. Tchem is based on Sandia National Laboratories' explosive chemistry code Xchem [6]. Tchem includes adaptive gridding, multiple phase changes, volumetric source terms, enclosure radiation, and contact resistance. The energy equation solved by Tchem is $\rho c(\partial T/\partial t) + \nabla \cdot q = -Q\rho(\partial F/\partial t)$, where ρ, c, T, q, Q, and F represent material density, specific heat, temperature, conductive energy flux using Fourier law ($q = -k\nabla T$, with k being thermal conductivity), energy release, and unreacted fraction. Table 1 summarizes the equations used in the diffusion model. An algorithm for implementing the model is given in the footnotes of Table 1. The algorithm accounts for the initial mixed "s_i" layer that forms before ignition. Table 2 gives the parameters for the diffusion model. Table 3 gives thermophysical properties for the Co/Al system discussed in the current work. The properties of the intermetallic were determined with common mixture rules, e.g. the specific heat is mass fraction weighted and the thermal conductivity is volume fraction weighted.

The bilayer material is partially melted as the temperature increases to the melting point of Al. The remainder of the bilayer material liquefies when the melting point of the cobalt is exceeded, although not all designs reach this temperature. The bilayer material no longer is composed of separate materials

Table 1: Auxiliary equations used in the continuum diffusion model†.

a	Thickness of material A	$a = \dfrac{a_o + b_o - s}{1 - \dfrac{\rho_A}{\rho_B}\dfrac{M_{w,B}}{M_{w,A}}\dfrac{N_B}{N_A}}$	(1)
b	Thickness of material B	$b = a\dfrac{\rho_A}{\rho_B}\dfrac{M_{w,B}}{M_{w,A}}\dfrac{N_B}{N_A}$	(2)
s	Thickness of reacted layer	$\dfrac{ds}{dt} = \dfrac{Dw}{s}$, where $w = (1 + b_o / a_o)$	(3)
F	Unreacted fraction	$F = 1 - \dfrac{s}{a_o w}$ and $\dfrac{dF}{dt} = -\dfrac{D}{a_o s}$	(4)
ρ	Density of multi-layer foil	$\rho = \rho_{AB} = \dfrac{a_o\rho_A + b_o\rho_B}{a_o + b_o}$	(5)
D	Diffusion coefficient	$D = D_o \exp\left(-\dfrac{E}{RT}\right)$	(6)

†Algorithm for implementing model:

a) Choose a_o, calculate b_o using (2).
b) Choose s_i (this is the *initial* premixed layer that forms prior to ignition).
c) Calculate a_i using s_i and (1).
d) Calculate b_i using (2).
e) Calculate F_i using s_i and (4).
f) Solve ordinary differential equations in (3) and (4) for s and F.

Table 2: Diffusion model parameters.

Property	Description	Co/Al*
s_i, m	Initial mixed layer thickness	2.5×10^{-9}-2.9×10^{-9}
D_o, m^2/s	Initial diffusion coefficient	4.5×10^{-10}-5.5×10^{-9}
E/R, K	Activation Energy/gas constant	5035.8

*Ranges are assumed to be uniformly distributed.

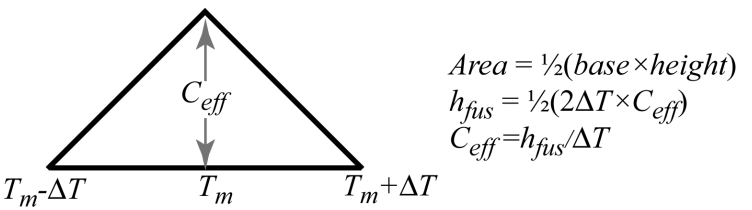

Figure 3: The area of the triangle is the latent enthalpy of fusion. The effective heat capacity is the height of the triangle with the base of the triangle equal to the temperature interval of the mush zone, e.g. 2ΔT.

once the material has reacted, e.g. $F = 0$. Solidification of the intermetallic occurs in two steps using the dual enthalpies of fusion in Table 3. Phase change is modelled using an effective capacitance model [7] with a mush zone as shown in Figure 3. The effective heat capacity at the melting point is the latent enthalpy divided by ΔT as shown in Figure 3. The specific heat is held constant until $T_m - \Delta T$. The specific heat is then increased linearly with temperature to a value of $c + c_{eff}$ at T_m. The specific heat is then decreased linearly to a value of c at $T_m - \Delta T$. The effective capacitance model is used for both phase changes.

Table 3: Thermophysical properties of Al, Co, and Co/Al[a].

Property	Al	Co	Co/Al
c, J/kgK	888–906	417–425	565–576
h_f, J/g	0	0	-1,260 to -1,400
h_{fus}, J/g	397	273	125, 187
k, W/mK	213–261	90–110	164–201
M_w, g/mol	27.0	58.9	85.9
ρ, g/cm^3	2.70	8.86	5.16
T_m, K	934	1770	934, 1770

[a]All properties except heats of formations, h_f, are from reference [8]. Heats of formation are from reference [9]. Property ranges are assumed to be uniformly distributed. These ranges are used with the uncertainty predictions.
[b]The Co/Al foil is assumed to partially melt at the melting point of both the pure metals. The two latent enthalpies for the Co/Al foil are calculated as: $h_{fus,Co/Al} = h_{fus,Al}(M_{w,Al} / M_{w,AlCo})$ and $h_{fus,Co}(M_{w,Co} / M_{w,AlCo})$.

An efficient *constrained sampling* technique known as Latin hypercube sampling (LHS) was used to determine the sensitivity of the predicted front velocities to uncertainty in the eight (8) input parameters: k_{Al}, c_{Al}, D_o, s_o, k_{Co}, c_{Co}, ΔT, and h_{rzn}. All of these parameters except ΔT are listed in Tables 2 and 3 with an assumed uniform distribution. ΔT is assumed to vary uniformly from 4-5 K. The LHS technique developed by McKay et al. [10] selects n different values for each of the 8 uncertain variables. In the current work, the number of samples, n, was chosen to be 9. The range of each input parameter was divided into n nonoverlapping intervals based on equal probability. One random value from each interval was selected according to a uniform probability density function in the interval. The n values were then paired in a random manner with the n values of the other parameters. The front velocities were then calculated n times with the n different sets of input parameters. The mean and standard deviation of the velocities were then calculated from the n sets of responses.

The relative importance of each model parameter to the uncertainty in the predicted front velocity was calculated by fitting a simple model to the 9 LHS runs, $v = A_0 + A_1 k_{Al} + ... + A_8 E / R$, and using a mean value analysis to determine the importance. The coefficients, A_i, were determined by setting up 9 equations

with 9 unknown coefficients and solving for the coefficients. The derivatives of V, with respect to input parameters i are the sensitivity coefficients, which are also the regression coefficients, *e.g.* $\partial V/\partial k_{Al} = A_1$. The variance of the velocity, sensitivity coefficients, and importance factors are then:

$$\sigma_V^2 = \sum_{i=1}^{8} \left(\sigma_i A_i\right)^2 \ , \ \gamma_i = \frac{\sigma_i}{\sigma_T} \times A_i \ , \text{ and importance} = \gamma_i^2 \ \text{ with } \sum_{i=1}^{8} \gamma_i^2 = 1 \, .$$

3 Results

The speed of the steady-state reaction front depends on the bilayer thickness as shown in Figure 4. The thick black line in Figure 4 is the arithmetic average of the 9 LHS samples. The gray area represents the 95% LHS confidence interval of the velocity prediction. The 95% uncertainty in the data varies from ±0.05 to ±0.3 m/s (depending on multilayer geometry) and ±3 nm representing two standard deviations. For example, a bilayer thickness of 10 nm resulted in a predicted front velocity 5-8 m/s. As the bilayer thickness was increased, the front velocity increased to 6-10 m/s at the $t_{b,max}$ thickness of ~15 nm as shown in Figure 4. The front velocity decreased with increasing bilayer thickness when $t_b > t_{b,max}$. Most of the data were within the LHS confidence interval. The velocity of the datum point above 80 nm was less than the model prediction. The mean of the data points near $t_{b,max}$ were also outside of the 95% predicted LHS confidence interval. More work is needed to address these extreme points. Temperature dependent thermophysical properties are probably necessary for better agreement as temperatures range from 300 K to 2000 K. The front may be driven by the ignition source causing more uncertainty for thin bilayer thicknesses near t_{bc}.

Figure 5 shows the parameters that contribute to the uncertainty in the velocity prediction. The percent perturbation about the mean is also given in Figure 5. Since detailed information about the scatter in the eight input parameters is unknown, a simple uniform distribution was assumed. The uncertainty in the predicted velocity is based on the assumed distribution and magnitude of the scatter about each of the eight parameters. The actual scatter may be more or less than the values given in Figure 5. The three parameters that contribute to the uncertainty in the burn velocity prediction are the heat of reaction, diffusion coefficient, and the thermal conductivity of Al. The uncertainty in liquid aluminium is likely higher than the range studied here. For example, the Al thermal conductivity decreases to about 93 W/mK [12] upon melting. Furthermore, the specific heat of Al increases from 897 to 1150 J/kgK as temperature increases from 300 to 800 K [11]. Clearly, temperature dependent properties should be considered for future work.

Figure 6 shows a few of the temperature profiles from 0.05 to 0.5 ms after ignition of a free standing foil with a bilayer thickness of 100 nm.

A constant temperature boundary was used to initiate the Co/Al nanolaminate. The temperature of the left-hand boundary was set to a constant value of 800 K, which was 134 K below the melting point of the aluminium. As the energy was conducted into the foil, the exothermic reaction of Al with Co

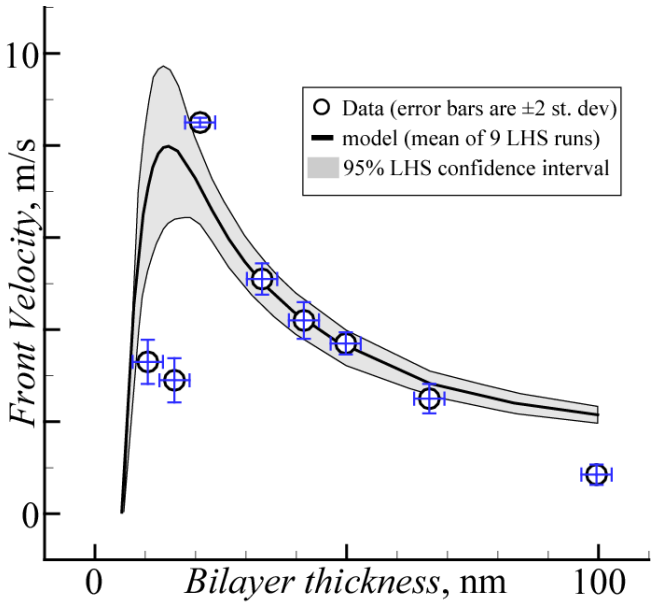

Figure 4: Effect of bilayer thickness on burn front speed. The black line is the mean of 9 LHS simulations. The gray area is the 95% LHS confidence interval. Symbols are measurements with error bars.

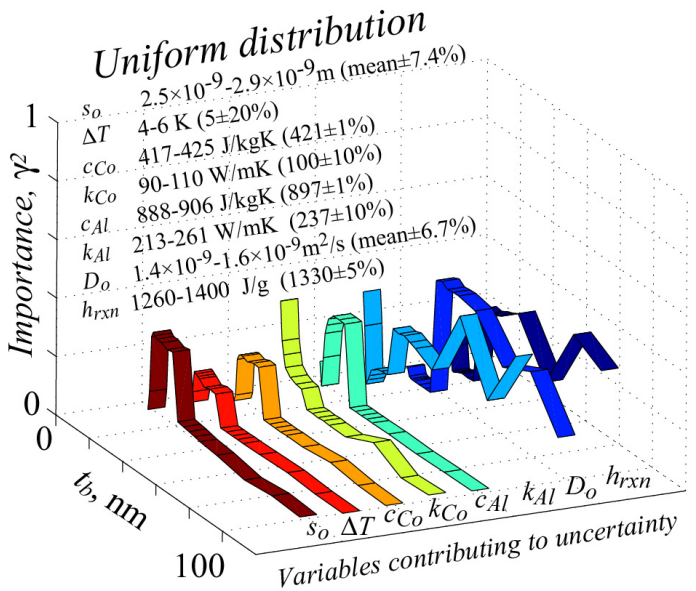

Figure 5: Parameters that contribute to uncertainty in velocity prediction.

caused the temperature to increase above the boundary temperature at 0.05 ms. At 0.2 ms, the exothermic reactions were sufficient to completely melt the aluminium. At 0.27 ms, the temperature rise was sufficient to exceed the melting point of the cobalt. The temperature profiles level out at the melting point of both the aluminium and the cobalt. At steady-state, the temperature rises from 300 K to about 2070 K. The time step used for these "stiff" calculations was 0.1×10^{-9} s.

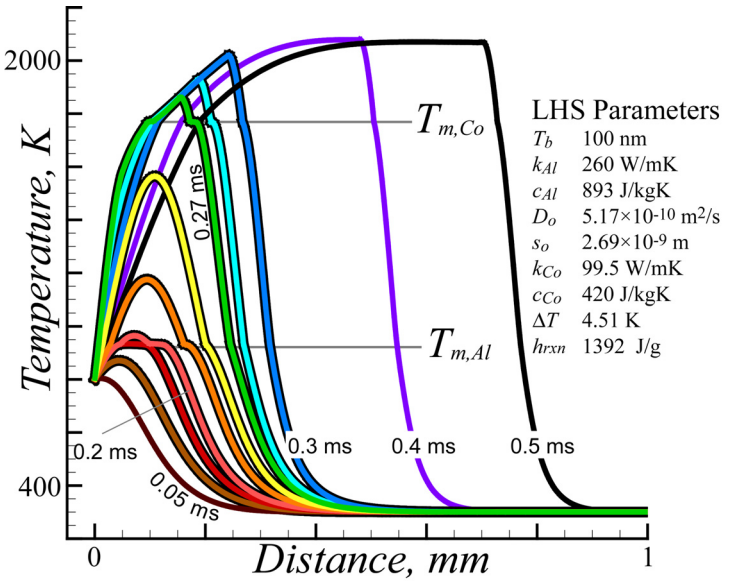

Figure 6: Temperature profiles from 0.05 to 0.5 ms after ignition of a Co/Al nanolaminate with a bilayer thickness of 100 nm.

The front profiles depicted in Figure 6 do not show oscillatory behaviour (i.e. periodic fluctuations in temperature with distance). However, for certain parameter sets, oscillatory behaviour was observed in the temperature profiles. Oscillatory behaviour was most noticeable when the reaction energy was low, such as for thin bilayers. Figure 7 shows temperature oscillations ranging from 1290 to 1294 K for a system with 10.7 nm bilayers. The period of the oscillations was about 100 μm. For a bilayer thickness of 10.7 nm, more than 50% of the bilayer is composed of the premixed Co_xAl_y phase leaving the nanolaminate without sufficient reactants to continue the exothermic temperature increase. Other modes of oscillation related to latent effects have been observed, e.g. the temperature excursions are halted when the melting point is reached. Oscillatory behaviour in exothermic nanolaminates has also been reported by Jayaraman et al. [13].

A rippled surface morphology has been discovered in reacted Co/Al foils (after cool down). Although this could be the result of several different mechanisms, it is intriguing that the structural periodicity is similar to that predicted from modelling. Figure 7 shows a scanning electron micrograph of the surface morphology of a reacted Co/Al foil.

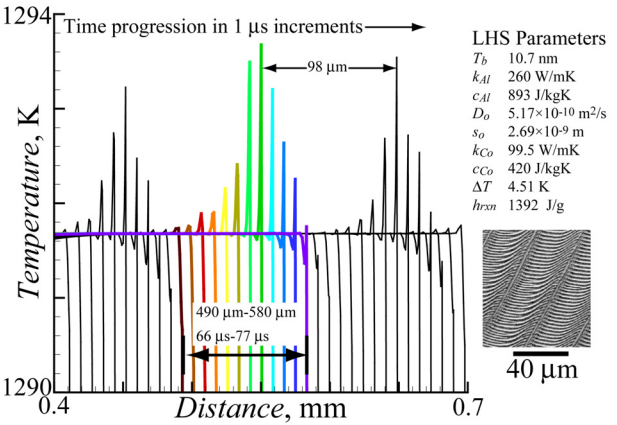

Figure 7: Temperature profiles from 56 to 91 μs after ignition of a Co/Al nano-laminate with a bilayer thickness of 10.7 nm. The scanning electron micrograph (bottom right) shows the post reaction foil surface morphology for a bilayer of 66.4 nm and total thickness of 7.5 μm.

4 Summary and conclusions

The diffusion-limited model of Hardt and Phung [5] has been used with a simple phase-change model to simulate the self-sustained, high temperature front propagation of Co/Al nanolaminates. The model utilizes a stiff ODE solver with adaptive gridding. Both steady and oscillatory front behaviours were predicted. The oscillatory behaviour was most prominent for small bilayer thickness where more than half of the bilayer was composed of a premixed Co_xAl_y layer. This finding is consistent with predictions by Jayaraman et al. [13] for Ni/Al nanolaminates. The dependence of the front velocity on the bilayer thickness has been predicted and compared to experiments. The uncertainty of the front velocity to various model parameters was also determined with the most sensitive parameters being the reaction enthalpy, diffusion coefficient, and thermal conductivity of the Al. The measured front velocities for a large range of bilayer thicknesses up to 80 nm are within the 95% LHS prediction interval. However, the model indicated that the front velocities for bilayer thicknesses above 80 nm were faster than measured front velocities. Differences may be due to using constant thermophysical properties for Co/Al. Future work will address temperature dependent properties and other foil compositions.

Acknowledgements

Sandia is a multiprogram laboratory operated by Sandia Corporation, a Lockheed Martin Company, for the United States Department of Energy under Contract DE-AC04-94AL85000. The authors appreciate the technical assistance of Eric

Jones, Jr. We are thankful to Mel Baer for suggesting the use of the Hardt and Phung [5] diffusion model. We are also thankful for comments from internal reviewers at Sandia National Laboratories, Rob Sorensen and Bill Erikson.

References

[1] Wang, J., Besnoin, E., Knio, O.M., Weihs, T.P., Effects of physical components on reactive nanolayer joining. *Journal of Applied Physics*, **97**, pp. 114307(1)-7114307(7), 2005.

[2] Adams, D.P., Hodges, V.C., Bai, M.M., Jones, E. Jr., Rodriguez, M.A., Buchheit, T., and Moore, J.J., Exothermic Co/Al nanolaminates. *Journal of Applied Physics*, in review.

[3] Wickersham, C.E., and Poole, J.E., Explosive crystallization in zirconium silicon multilayers. *J. Vac. Sci. Technol. A, **6(3)**, pp. 1699–1702, 1988.*

[4] Hobbs, M.L. and Adams, D.P., Reactive nano-films of Al and Pt. *Proceedings of the 8th World Congress on Computational Mechanics*, Venice, Italy, June 30-July 5, 2008.

[5] Hardt, A.P. and Phung, P.V., Propagation of gasless reactions in solids—I. Analytical study of exothermic intermetallic reaction rates. *Combustion and Flame*, **21**, pp. 77–89, 1973.

[6] Gross, R.J., Baer, M.R., and Hobbs, M.L., XCHEM-1D: a heat transfer-chemical kinetic computer program for multilayered reactive materials. Sandia National Laboratories Report SAND93-1603, 1993.

[7] Yao, L.S. and Prusa, J., Melting and freezing. *Advances in Heat Transfer*, **19**, Hartnett JP and Irvine TR Jr., editors (1989).

[8] Lide, D.R., editor-in-chief, CRC Handbook of Chemistry and Physics 88th Edition 2007-2008, CRC Press, Cleveland, Ohio, 2008.

[9] de Boer, F.R., Boom, R., Mattens, W.C.M., Miedema, A.R., and Niessen, A.K., Cohesion in Metals Transition Metal Alloys, Elsevier Science Publishers, North-Holland Physics Publishing, Amsterdam, 1988.

[10] McKay, M.D., Conover, W.J., and Beckman, R.J. A comparison of three methods for selection values of input variables in the analysis of output from a computer code. *Technometrics*, **22(2)**, p. 239, 1979.

[11] Incropera, F.P. and DeWitt, D.P., *Fundamentals of Heat and Mass Transfer*, 5th Edition, John Wiley & Sons, New York, 2002.

[12] Weast, R.C., Editor. CRC Handbook of Chemistry and Physics 55th Edition. CRC Press, Cleveland, Ohio, p. E10, 1974.

[13] Jayaraman, S., Knio, O.M., Mann, A.B., and Weihs, T.P., Numerical predictions of oscillatory combustion in reactive multilayers. *Journal of Applied Physics*, **86(2)**, pp. 800–809, 1999.